

## Physicochemical properties and NH<sub>3</sub>-SCR catalytic performance of intercalated layered aluminosilicates

Agnieszka Szymaszek-Wawryca<sup>1</sup>, Urbano Díaz<sup>2</sup>, Bogdan Samojedon<sup>1</sup>, Monika Motak<sup>1</sup>

<sup>1</sup> Faculty of Energy and Fuels, AGH University of Science and Technology, al. A. Mickiewicza 30, 30-059 Kraków, Poland

<sup>2</sup> Instituto de Tecnología Química, Universitat Politècnica de València - Consejo Superior de Investigaciones Científicas, Avd. de los Naranjos s/n, 46022 Valencia, Spain

Corresponding author: agnszym@agh.edu.pl (Agnieszka Szymaszek-Wawryca)

**Abstract:** The representative of natural layered clays, bentonite, was modified according to two routes and tested as a new catalyst for selective catalytic reduction of nitrogen oxides with ammonia (NH<sub>3</sub>-SCR). The natural acid-activated clay was ion-exchanged with Na<sup>+</sup> or remained in H-form and pillared with metal oxides. In order to limit the number of synthesis steps, iron as an active phase was introduced simultaneously with Al<sub>2</sub>O<sub>3</sub> during the intercalation procedure. Additionally, the samples were doped with 0.5 wt% of copper to promote low-temperature activity. It was found that the performed modifications resulted in disorganization of the ordered layered arrangement of bentonite. Nevertheless, acid activation and pillaring improved structural and textural parameters. The results of catalytic tests indicated that the samples containing Fe<sub>2</sub>O<sub>3</sub> pillars promoted with Cu exhibited the highest NO conversion of 85% at 250 °C (H-Bent-AlFe-Cu) and 75% at 300 °C (Na-Bent-AlFe-Cu). What is important, activity of the protonated samples in the high-temperature region was noticeably affected by the side reaction of ammonia oxidation, correlated with the production of NO and resulting in N<sub>2</sub>O emission during the process comparing to Na-Bentonite catalysts.

**Keywords:** bentonite, DeNO<sub>x</sub>, pillaring, iron, copper

### 1. Introduction

Selective catalytic reduction with ammonia (NH<sub>3</sub>-SCR) is a widely used technology to abate the extensive emissions of nitrogen oxides (NO<sub>x</sub>) (Skalska et al., 2010). In fact, the method provides satisfactory efficiency, nevertheless, there are some important operational problems related to the industrial catalyst, V<sub>2</sub>O<sub>5</sub>-TiO<sub>2</sub> promoted with MoO<sub>3</sub> or WO<sub>3</sub>. The great number of studies confirmed that the commercial catalytic system is very sensitive for the presence of alkali metals and SO<sub>2</sub> in the exhaust gas, moreover, it exhibits satisfactory activity only in a narrow temperature window (Szymaszek et al., 2020). Additionally, vanadium, which is the principal component of the catalyst, was classified as an environmentally-dangerous (Watt et al., 2018). Therefore, it is crucial to find a new and ecological-friendly catalyst of NH<sub>3</sub>-SCR. Among the number of potential precursors of the substitutive catalytic systems, the layered aluminosilicates seem to be the most promising. One of the greatest advantages of the materials is that they can be easily engineered and adopted for the number of important catalytic applications or sustainable chemical and biological processes. As a consequence, in the recent years, two-dimensional inorganic compounds with layered structures (layered clays) have attracted an increasing attention of the industries.

Natural layered materials occur commonly in the environment, thus, are relatively cheap and easy to acquire (Zhou, 2011a). Furthermore, the number of studies described successful reflection of the lamellar structure on the laboratory scale (Chlubná et al., 2012; Yamamoto et al., 2021; Zi et al., 2020). Thus, layered materials can be divided into natural and synthetic, hence, their physicochemical properties can be modified or tailored from the ground up. Typically, natural lamellar clays are composed of crystalline, aluminosilicate layers with the thickness of ca. 1 nm. One layer can be built of one (1:1 type) or two (2:1 type) Si-O sheets of tetrahedral geometry and one Al-O sheet of octahedral

geometry. Hence, in the case of 1:1 type, each layer consists of one Si-O and one Al-O sheet (T-O layer), while 2:1 type is characterized by the presence of one Al-O, chemically-bonded with two Si-O sheets (T-O-T layer). Stability of the entire aluminosilicate structure is provided by the weak, physical Van der Waals forces. The interlayer space of the materials is filled with water molecules and positively-charged ions, such as  $\text{Na}^+$ ,  $\text{K}^+$ ,  $\text{Ca}^{2+}$ , and  $\text{Mg}^{2+}$ . In general, the presence of the cations compensates the negative charge of the aluminosilicate layers caused by partial substitution of metal ions, for example  $\text{Mg}^{2+}$  and  $\text{Al}^{3+}$  in the octahedral or  $\text{Al}^{3+}$  and  $\text{Si}^{4+}$  in the tetrahedral sheets (Szymaszek et al., n.d.; C. H. Zhou, 2011b)(Szymaszek et al., n.d.; C. H. Zhou, 2011b)(Szymaszek et al., n.d.; C. H. Zhou, 2011b)(Szymaszek et al., n.d.; C. H. Zhou, 2011b). The interlayer cations provide superior ion-exchange properties of clays and enable to modify their chemical composition and morphological features by the incorporation of various molecules into the interlayer space (Yamamoto et al., 2021).

One of the representatives of natural layered clays is bentonite, characterized by T-O-T structure. Bentonite consists mainly of montmorillonite, which is classified as dioctahedral smectite. The tetrahedral and octahedral sheets of bentonite are occupied by  $\text{Si}^{4+}$  and  $\text{Al}^{3+}$  cations, respectively, wherein  $\text{Al}^{3+}$  is frequently substituted with  $\text{Mg}^{2+}$  and/or  $\text{Fe}^{3+}$  (Kumar & Lingfa, 2020; Paluszkiwicz et al., 2008). Since the great majority of bentonites are formed from weathering of volcanoclastic rocks, apart from montmorillonite, the clays usually contain some amounts of quartz, pyrite, cristobalite, kaolinite, and mica (De Oliveira et al., 2016; Szymaszek et al., n.d.). The structural and chemical characterization and high mechanical and chemical stability of bentonite combined with its abundance in the environment makes the material highly-valued for many practical applications. Therefore, raw and modified bentonites were used i.e. in the adsorption of dyes (Adeyemo et al., 2017; Özcan & Özcan, 2004) or pesticides (Shattar et al., 2020), removal of heavy metals (Lin et al., 2021; Zanin et al., 2017), or catalytic oxidation reactions (Carriazo et al., 2007).

In general, there are many types of bentonite deposits occurring in nature and the great majority exhibits rather low specific surface area ( $S_{BET}$ ) of 20-130  $\text{m}^2 \cdot \text{g}^{-1}$  (Shattar et al., 2020). Since the parameter is crucial for the industrial applications of the clay, numerous studies were conducted to increase  $S_{BET}$  and improve textural characteristics of bentonites. One of the most advantageous methods to enhance structural properties of natural clays is activation with mineral acids (such as sulfuric, hydrochloric, or nitric) (Komadel, 2016; Motak, 2008; Stawiński et al., 2016). During the modification, the material is dissolved in the acidic medium and di- or trivalent cations are replaced with monovalent protons, originating from the molecules of acid. As a consequence, the majority of ferrous, ferric, aluminum, and magnesium cations are removed from the clay, simultaneously with undesired impurities. It was reported that in most cases the octahedral layer of the clay is attacked first by the hydrogen cations to generate more acidic Si-rich phase (Shattar et al., 2020). Therefore, acid treatment is normally performed to alter the smectite layers, increase surface crystallinity, specific surface area (even up to 200  $\text{m}^2 \cdot \text{g}^{-1}$ ), and functionalities of bentonites. The elimination of metal ions from the clay lattice and thus, partial delamination significantly influences on the acidic character of the material. The acid sites in the pretreated samples can be situated in two positions: on the easily-accessible external layered, opened-up by delamination and in the residual laminal regions, not available without prior swelling of the clay (Hart & Brown, 2004). Additionally, there are two types of acid centers in the modified clays, wherein their respective concentration depends on the hydration degree of the material. The generation of the Brønsted acid centers is related to the low chemical stability of the protonated clays and auto-transformation based on the incorporation of  $\text{Al}^{3+}$  cations into ion-exchange sites (Rhodes & Brown, 1995). Further hydrolysis of the clay results in the hydration of aluminum cations and generation of Brønsted acid sites, strongly influenced by the content of  $\text{H}_2\text{O}$  molecules. In contrast, Lewis acidity predominates in the dehydrated clays and its strength can be optimized by the type of exchangeable cations (Hart & Brown, 2004). The effects of the modification of natural aluminosilicates with acids was widely described in the literature in recent years. Maged et al. (Maged et al., 2020) compared the potential of raw and acid-modified bentonite for the adsorption of ciprofloxacin and its removal from aqueous solution. The authors also investigated the influence of various conditions of the activating agent (HCl) on the structural properties of the material. It was found that pretreatment with acid did not change mesoporous character of bentonite, however, doubled the  $S_{BET}$  and increased the total pore volume. The improvement of the textural features were ascribed to splitting of the clay particles within

the octahedral sheets. Moreover, higher value of the specific surface area observed for the pretreated sample was attributed to decreased pore diameter. Acid-treated natural layered clays were also examined as the catalysts of  $\text{NH}_3$ -SCR. Motak (Motak, 2008) studied the catalytic potential of modified montmorillonite for NO reduction and assumed that activation of the material with HCl contributed to the formation of surface acidic groups, which facilitated distribution of the metallic active centers within the catalyst. The research carried out by Chmielarz et al. (Chmielarz et al., 2010; Chmielarz, Rutkowska, et al., 2014; Lucjan Chmielarz et al., 2012) confirmed that leaching of natural clay (vermiculite) with acids activates the material in  $\text{NH}_3$ -SCR and high-temperature decomposition of  $\text{N}_2\text{O}$ . According to the authors, concentration of acid and duration of the pretreatment are the crucial factors determining the final physicochemical properties of the catalyst.

Apart from acid activation, natural layered clays can be modified by intercalation (pillaring) with guest species. The procedure is based on the introduction of so-called "pillars" into the interlayer space and can be performed after pretreatment of the clay with acid (Chmielarz et al., 2009; Motak, 2008). The pioneering research on the intercalation procedure described pillaring with amines and it was found that organic molecules are thermally decomposed above  $250\text{ }^\circ\text{C}$  (Bergaya et al., 2006). Hence, further investigations were focused on the intercalation with metal oxides, such as Al, Zr, Ti, Fe, Ce or their mixtures (Catrinescu et al., 2012; Gil et al., 2013). In general, the pillaring procedure assumes replacement of the interlayer cations of the clay by large polynuclear cationic species, present in the pillaring solution. Thermal treatment conducted after intercalation yields metal oxides which increase the lamellar spacing, specific surface area, and porosity of the clay (Bertella & Pergher, 2015). Due to the fact that the introduced metal oxide pillars are easily-accessible through the 2D clay structure, the choice of the intercalating agent usually depends on the desired properties of the material. The influence of intercalation on the structural features of layered aluminosilicates was extensively investigated over the past years (Chmielarz et al., 2018; Chmielarz, Kowalczyk, et al., 2014; Grzybek, 2007). It was confirmed that the specific surface area can increase from  $30\text{ m}^2 \cdot \text{g}^{-1}$  to  $279\text{ m}^2 \cdot \text{g}^{-1}$  after introduction of the metal oxide species (Chmielarz, Kowalczyk, et al., 2014). According to the literature, the pillared clays exhibit very high potential as the catalysts of  $\text{NH}_3$ -SCR. Chen et al. (Chen et al., 2016) intercalated natural montmorillonite with  $\text{Al}_2\text{O}_3$  and  $\text{Al}_2\text{O}_3\text{-Cr}_2\text{O}_3$  and tested the materials as the catalysts for NO reduction with ammonia after modification with manganese. It was observed that aluminum assists in the stabilization of the chromium oligocations and co-existence of  $\text{Al}_2\text{O}_3$  and  $\text{Cr}_2\text{O}_3$  yields higher specific surface area and better  $\text{NH}_3$ -SCR catalytic performance within  $140\text{-}300\text{ }^\circ\text{C}$ . Han et al. (Han et al., 2019) compared the catalytic performance in NO reduction of Mn-montmorillonite intercalated with  $\text{Cr}_2\text{O}_3$ ,  $\text{ZrO}_2$ , or  $\text{Fe}_2\text{O}_3$  and found that pillaring with iron oxide resulted in the formation of new acidic centers which promote adsorption of ammonia. As a result, the clay pillared with  $\text{Fe}_2\text{O}_3$  exhibited the highest NO reduction in the low-temperature region. Additionally,  $\text{Fe}^{3+}$  centers were reported to decrease the production of nitrous oxide during  $\text{NH}_3$ -SCR. Moreover, in contrast to Chen et al. (Chen et al., 2016), the authors reported that pillaring of Mn-modified montmorillonite with chromium oxide promotes formation of  $\text{N}_2\text{O}$ , which is non-desired product of  $\text{NH}_3$ -SCR. The authors ascribed this effect to strongly oxidative character of chromium. Last, but not least, natural solid materials, including modified layered clays can be easily recovered after the catalytic reaction, for example by the well-known flotation (Shen et al., 2023; Zhao et al., 2023). The most important advantage of this procedure is that its cost in the majority of cases is significantly lower comparing to the replacement of the spent catalysts by the newly-purchased system.

Despite the fact that acid-pretreated and pillared layered clays were confirmed to exhibit satisfactory  $\text{NH}_3$ -SCR catalytic performance, there are still some challenges related to the preparation of the effective catalytic system supported on these natural materials. First of all, the great majority of studies used strongly oxidizing manganese as an active phase, which promotes  $\text{NH}_3$  oxidation, thus, consumption of the reducing agent, and finally lower NO reduction. On the other hand, it was reported that both  $\text{Al}_2\text{O}_3$  and  $\text{Fe}_2\text{O}_3$  pillars contribute to the generation of new acid centers, moreover,  $\text{Fe}^{3+}$  itself acts as a catalyst for NO reduction. Therefore, the simultaneous presence of aluminum and iron oxide seems to be a good idea to increase the catalytic potential of a layered clay. What is more, since the number of studies confirmed synergistic effect of copper and iron in  $\text{NH}_3$ -SCR catalysts (Boroń et al., 2015; Ibrahim et al., 2021; Zhang et al., 2014), copper would be a good alternative to the toxic vanadium present in the

commercial system or highly-oxidative manganese, used usually in the previously studied montmorillonite-supported catalysts.

To the best of our knowledge, acid-modified and  $\text{Al}_2\text{O}_3\text{-Fe}_2\text{O}_3$ -pillared bentonite with Cu as an active phase has never been tested as a catalyst of  $\text{NH}_3$ -SCR. Therefore, in this work we prepared such material and compared it to the sample pillared with  $\text{Al}_2\text{O}_3$  in order to determine the impact of iron oxide pillars on the catalytic performance.

## 2. Materials and methods

The bentonite supplied by ZGM Zębiec SA (Zębiec, Poland) was used as a raw material for the preparation of a series of the catalysts supported on natural layered clays. The non-modified material was labeled as Bent.

In the first step, raw bentonite was added to the solution of nitric acid (Avantor Performance Materials Poland S. A., Gliwice, Poland) (2 M) with a clay mass/acid volume ratio of 1 g/10 cm<sup>3</sup> and activated at 105 °C for 24 h. After that time, the material was filtered, washed several times with distilled water, dried at 100 °C overnight, and calcined at 500 °C for 5 h. The acid-modified precursor was labeled as H-bent. In order to investigate the influence of the presence of interlayer cations on the efficiency of intercalation, a part of H-Bent was transformed into the sodium form by the treatment with the solution of  $\text{NaNO}_3$  (Avantor Performance Materials Poland S. A., Gliwice, Poland) (1 M). The sodium-bentonite was labeled as Na-bent.

Intercalation of H-bent and Na-bent with  $\text{Al}_2\text{O}_3$  was performed by ion-exchange method, using an aluminum hydroxy-oligomeric solution obtained according to the reproduced method proposed by Barth et al. (Barth et al., 2004). Typically, an adequate volume of NaOH (Avantor Performance Materials Poland, Gliwice, Poland) solution (0.4 M) was added dropwise to  $\text{Al}(\text{NO}_3)_3 \cdot 9\text{H}_2\text{O}$  (Eurochem BGD Sp. z o. o., Tarnów, Poland) solution (0.4 M) maintained under stirring, until the molar ratio of  $\text{OH}/\text{Al} = 2.4$  was reached. The pillaring solution was agitated at 60 °C for 12 h and subsequently aged at room temperature for 5 days.

Intercalation of H-bent and Na-bent with  $\text{Al}_2\text{O}_3\text{-Fe}_2\text{O}_3$  was carried out by ion-exchange method reported by Muñoz et al. (Muñoz et al., 2017). The solution of  $\text{Fe}^{3+}$  and  $\text{Al}^{3+}$  cations derived from  $\text{Al}(\text{NO}_3)_3 \cdot 9\text{H}_2\text{O}$  and  $\text{Fe}(\text{NO}_3)_3 \cdot 9\text{H}_2\text{O}$  (Firma Chempur, Piekary Śląskie, Poland) in which the molar ratio of  $\text{Fe}^{3+}/(\text{Fe}^{3+} + \text{Al}^{3+}) = 0.2$ , whereas the total concentration of trivalent ions was 0.4 M. The preparation of the solution was performed by slow addition of NaOH solution (0.4 M) to the continuously stirred solution of the trivalent cations, until  $\text{OH}/\text{Me}^{3+}$  molar ratio reached 2.0. The resulting liquid, clear product was aged at room temperature for 72 h.

The pillaring procedure was conducted by the slow addition of the pillaring solution (with Al- or Al-Fe oligocations) to 10 wt.% suspension of 5 g of the acid-activated bentonite in distilled water. The volume of the pillaring solution was calculated to obtain 24 mmol of  $\text{Al}^{3+}$  or  $\text{Al}^{3+}\text{-Fe}^{3+}$  per 1 g of the clay. The prepared mixture was stirred at 60 °C for 24 h, filtered and washed several times with distilled water. The obtained solid products were dried at 100 °C overnight and then calcined at 500 °C for 5 h. The samples were labeled as H-bent-Al and H-bent-AlFe for  $\text{Al}_2\text{O}_3$  and  $\text{Al}_2\text{O}_3\text{-Fe}_2\text{O}_3$ -pillared H-bent, respectively and Na-bent-Al and Na-bent-AlFe for  $\text{Al}_2\text{O}_3$  and  $\text{Al}_2\text{O}_3\text{-Fe}_2\text{O}_3$ -pillared Na-bent, respectively.

Copper as an active phase (or promotor in the case of iron-pillared aluminosilicates) was introduced by adsorption from the solution method by stirring of the modified bentonite or MCM-36 in the adequate volume of  $\text{Cu}(\text{NO}_3)_2 \cdot 3\text{H}_2\text{O}$  (WARCHEM Sp. z o. o., Marki, Poland) solution at 40 °C for 24 h, to obtain the Cu content of 0.5 wt.%. The list of the obtained catalysts and their precursors with the corresponding descriptions and codes are presented in Table 1.

## 3. Results and discussion

### 3.1. $\text{NH}_3$ -SCR catalytic performance

The bentonite samples with Fe or Fe and Cu were tested as the catalysts of selective catalytic reduction of NO with ammonia. Fig. 1. displays NO conversion obtained for the catalysts with the protonated- or

Table 1. Descriptions and codes of the investigated samples

Sample code	Description
Bent	Non-modified bentonite
H-bent	Bentonite activated with 2 M solution of HNO <sub>3</sub>
H-bent-Al	H-bent intercalated with Al <sub>2</sub> O <sub>3</sub>
H-bent-AlFe	H-bent intercalated with Al <sub>2</sub> O <sub>3</sub> -Fe <sub>2</sub> O <sub>3</sub>
H-bent-Al-Cu	H-bent-Al modified with Cu
H-bent-AlFe-Cu	H-bent-AlFe modified with Cu
Na-bent	H-bent transformed into sodium form
Na-bent-Al	Na-bent intercalated with Al <sub>2</sub> O <sub>3</sub>
Na-bent-AlFe	Na-bent intercalated with Al <sub>2</sub> O <sub>3</sub> -Fe <sub>2</sub> O <sub>3</sub>
Na-bent-Al-Cu	Na-bent-Al modified with Cu

sodium-form of the pillared bentonite. It can be observed that regardless the type of the support, the samples modified both with Cu and Fe were the most active. The highest NO conversion for H-Bent-AlFe-Cu (ca. 85%) and Na-Bent-AlFe-Cu (ca. 75%) was reached at 250 and 300 °C, respectively. Such result can be related to the synergy between iron and copper acting as an active phase of NH<sub>3</sub>-SCR catalysts. However, taking into consideration catalytically-beneficial dispersion of copper species (see UV-vis-DR outcomes), the promising activity of the samples can be ascribed mainly to Cu introduced into the materials. In the case of Na-Bent-Al-Cu and Na-Bent-AlFe-Cu, the conversion of NO was maintained on a stable level within 225-350 °C, while above this range started to gradually increase. In contrast, the activity of the protonated catalysts with Cu or Cu and Fe showed a decreasing trend in the high-temperature range. One of the possible reasons of this effect is oxidation of ammonia, thus its consumption and limited conversion of nitric oxide. Furthermore, H-Bent-AlFe and Na-Bent-AlFe exhibited the highest conversion within 400-450 °C. This effect is typical for iron-catalysts and results from the presence of more aggregated Fe<sub>x</sub>O<sub>y</sub> species. According to Brandenberger et al., low-temperature activity of Fe-catalysts is provided by the abundance in Fe<sup>3+</sup> isolated cations, while the activity in the middle- and high-temperature range results from the presence of Fe<sub>x</sub>O<sub>y</sub> oligocations. Therefore, since iron was introduced into bentonite exclusively in the form of metal oxide pillars, the characteristic high-temperature NO conversion of H-Bent-AlFe and Na-Bent-AlFe can be explained by the speciation of the active phase.

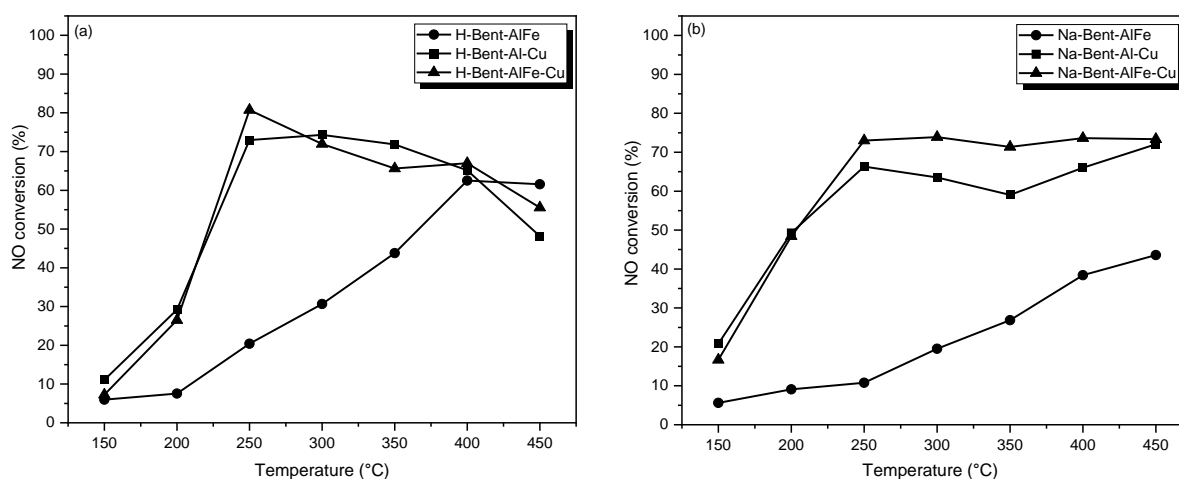
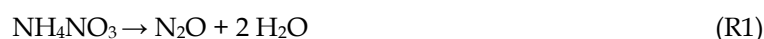


Fig. 1. NO conversion obtained for (a) H-bentonite-supported catalysts and (b) Na-bentonite-supported catalysts

The emission of nitrous oxide (a common by-product of NH<sub>3</sub>-SCR) during the catalytic reaction is one of the crucial factors determining the potential implementation of the catalyst on an industrial scale. The selectivity towards N<sub>2</sub>O for the investigated samples is presented in Fig. 2. In general, the production of nitrous oxide did not exceed 60 and 40 ppm for H-Bent- and Na-Bent-supported samples, respectively. Therefore, both groups of materials exhibit relatively low susceptibility to catalyze side reactions of NH<sub>3</sub>-

SCR. What is important, the emission of  $N_2O$  during the catalytic tests was determined by two factors: (1) type of the pillars and the active phase and (2) temperature of the reaction. In the case of H-Bent samples (Fig. 2(a).), generation of nitrous oxide increases linearly with temperature for H-Bent-AlFe and H-Bent-AlFe-Cu, while for H-Bent-Al-Cu it is maintained on a similar level within the entire temperature range. Therefore, one of the possible reasons for  $N_2O$  production for these samples is the presence of  $Fe_2O_3$  pillars. The opposite effect can be observed for Na-Bent-supported catalysts (Fig. 2(b).), since only Na-Bent-Al-Cu exhibited noticeable, gradual increase of nitrous oxide emission. Such result is most likely related to the activity of Cu-catalysts to oxidize ammonia above 350 °C. As already mentioned, temperature was the second crucial aspect influencing on  $N_2O$  selectivity of the materials. According to the general agreement, emission of nitrous oxide below 300 °C results from the thermal decomposition of ammonium nitrate species ( $NH_4NO_3$ ) formed on the catalyst surface during first steps of the catalytic process. Therefore, the generation of  $N_2O$  can be described by the following reaction (R1):



On the other hand, the formation of  $N_2O$  within 300-450 °C most likely originates from the presence of Lewis acid centers which participate in the oxidative dehydrogenation of  $NH_3$  and formation of  $NH$  species. Subsequently,  $NH$  reacts with  $NO$ , which further results in the generation of  $N_2O$ . Therefore, the highest concentration of  $N_2O$  detected for H-Bent-AlFe and H-Bent-AlFe-Cu can be correlated with better accessibility of the reacting molecules to the Lewis centers of the samples comparing to the others. This conclusion is supported by the highest specific surface area and superior total pore volume (cf. Table 2) among the investigated materials. Another reason of the generation of  $N_2O$  in the high-temperature range is oxidation of ammonia, which occurs commonly in the case of catalysts with transition metals as an active phase. According to Rahkamaa-Tolonen et al.  $NH_3$  oxidation reaction, which takes place above 350 °C contributes not only to the excessive formation of nitrous oxide, but also generation of additional portion of  $NO_2$  and  $NO$ . Thus, correlating the data presented in Fig. 1. and Fig. 2. it can be concluded that in the case of H-Bent catalysts oxidation of ammonia was more prominent comparing to Na-Bent. This assumption is supported by the decreasing  $NO$  conversion (caused by its generation from  $NH_3$  oxidation) combined with the gradually increasing  $N_2O$  concentration at high temperature.

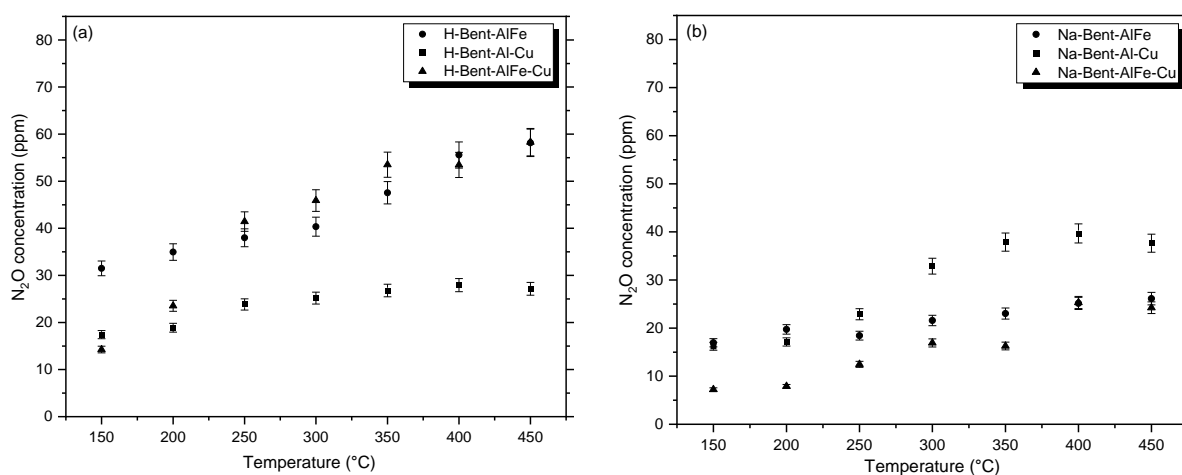


Fig. 2.  $N_2O$  concentration in the exhaust gas during the catalytic reaction performed for (a) H-bentonite-supported catalysts and (b) Na-bentonite-supported catalysts

### 3.2. Physicochemical properties of the materials

#### 3.2.1. Chemical composition

The chemical composition of bentonite before and after modifications was examined using ICP-OES and the obtained results are presented in Table 2. It can be observed that the content of the chemical elements in the raw clay is in agreement with that reported in the literature. Noteworthy, iron was naturally present in the structure of the material, which could potentially contribute to its activity in  $NH_3$ -SCR. As expected, after protonation, some significant amount of aluminum was removed from

bentonite. The dealumination phenomenon inducted not only hydrogenation of the material at the expense of  $\text{Al}^{3+}$ , but also removal of iron cations. What is more, according to Arus et al. pretreatment of bentonite with mineral acids results in the leaching of  $\text{Fe}^{2+}$  from the octahedral layer, which makes the species more affordable for the reacting molecules during catalytic reactions. Since the content of Al increased after intercalation with  $\text{Al}_2\text{O}_3$ , both H-bent-Al and Na-bent-Al were successfully pillared, which was also confirmed by XRD analysis. What is interesting, the efficiency of the introduction of  $\text{Al}_2\text{O}_3$  was higher for the sample without Na, which suggests that the interlayer hydrogen cations can be exchanged easier comparing to the sodium cations. On the other hand, while  $\text{Al}_2\text{O}_3$  was introduced simultaneously with  $\text{Fe}_2\text{O}_3$  pillars, the content of aluminum and iron was higher in the case of Na-bentonites. Therefore, the result of intercalation was strongly correlated with the type of interlayer ions present in the aluminosilicate. Additionally, the amount of  $\text{Na}^+$  significantly decreased after introduction of copper, regardless initial modification of bentonite. Last, but not least, the content of  $\text{Cu}^{2+}$  in the samples was very close to the intended one.

Table 2. Chemical composition of the materials determined by ICP-OES (in wt%)

Sample code	Si	Al	Na	Fe	Cu
Bent	21.60	9.65	< 0.01	1.43	< 0.01
H-Bent	36.68	2.99	< 0.01	0.30	< 0.01
H-Bent-Al	34.80	5.70	0.29	0.26	< 0.01
H-Bent-AlFe	33.68	2.59	0.27	8.63	< 0.01
H-Bent-Al-Cu	35.28	5.56	0.10	0.26	0.60
H-Bent-AlFe-Cu	33.93	2.61	0.11	8.63	0.55
Na-Bent	37.98	3.07	0.56	0.28	< 0.01
Na-Bent-Al	36.48	5.02	0.27	0.27	< 0.01
Na-Bent-AlFe	31.80	3.02	0.59	10.59	< 0.01
Na-Bent-Al-Cu	35.89	4.81	0.01	0.27	0.55
Na-Bent-AlFe-Cu	31.50	2.99	0.18	11.36	0.67

### 3.2.2. Textural properties

The porous texture and surface properties of the materials were analyzed using nitrogen adsorption-desorption measurements. The obtained isotherms are presented in Fig. 3., while the structural and textural characterization of the samples are collected in Table 3. The  $\text{N}_2$  sorption isotherm of non-modified bentonite was the type I according to IUPAC classification, characteristic for microporous solids with relatively low values of external surface area. Furthermore, the H4 hysteresis loop proved the presence of micro- and small mesopores in the aggregated particles of the raw bentonite. Hydrogenation procedure performed on the material did not influence its structural, nor textural parameters. In contrast, transformation of the sample into sodium form completely changed its characterization. It can be observed that Na-bent exhibited IV(a) isotherm with H3 hysteresis loop, hence ion-exchange with  $\text{Na}^+$  resulted in the formation of meso- and macroporous texture in the non-rigid aggregates of plate-like particles. After intercalation and introduction of Cu, all of the isotherms (except H-bent-Al) were of type IV(a), with a clear H3 hysteresis loop, thus, the presence of newly formed meso- and macroporosity. Basing on the sorption branch of H-bent-Al, it can be concluded that even after pillaring with  $\text{Al}_2\text{O}_3$  the sample preserved its microporous texture. Therefore, the texture of bentonite can be significantly changed exclusively upon the introduction of foreign ions of bigger radius or the mixture of various pillars and/or transition metals into the interlayer space and aluminosilicate framework, respectively.

As presented in Table 3, non-modified bentonite exhibited relatively high specific surface area in comparison to the data reported in the literature. However, one should note that characterization of the natural materials depends on their origin. Therefore, it can be assumed that the obtained result is fully correct and the bentonite used in the research can be treated as a representative sample. After acid activation,  $S_{\text{BET}}$  of the layered precursor was dramatically enhanced, confirming that pretreatment with mineral acids is an easy and effective approach to improve structural characterization of natural

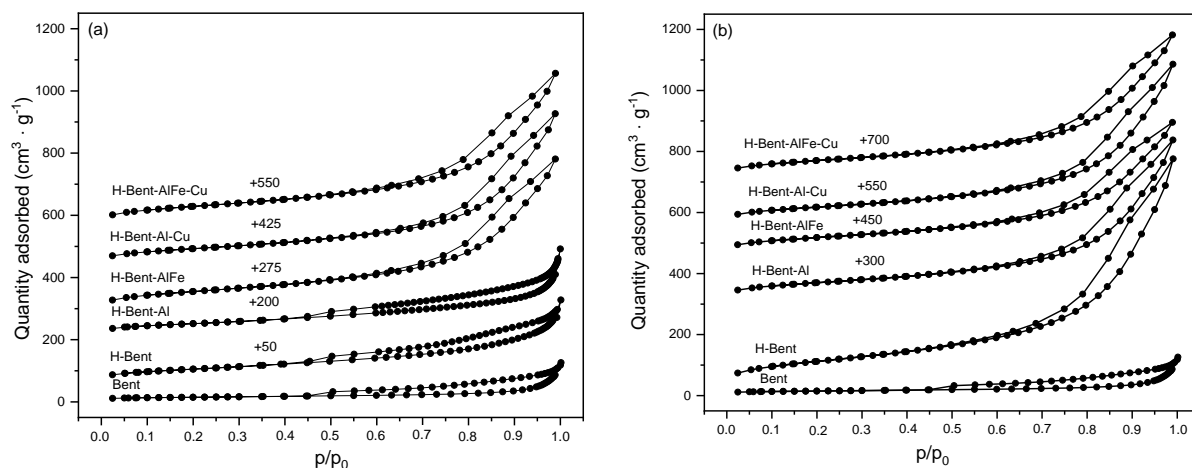


Fig. 3. N<sub>2</sub> sorption isotherms obtained for the investigated materials: (a) modified H-bent, (b) modified Na-bent (for better visibility, the adsorption branches were shifted by the values given in the figure)

aluminosilicates. Such effect is mainly caused by the replacement of metal cations with H<sup>+</sup> and removal of the impurities normally located near the pore openings in the natural clays. Additionally, transformation of the acid-treated material into the sodium form only slightly decreased its specific surface area. What is interesting, no regular trend regarding  $S_{\text{BET}}$  was observed in the case of the pillared and Cu-modified samples. Nevertheless, one can observe that regardless of the H- or Na-form of bentonite, the materials pillared with the mixture of Al<sub>2</sub>O<sub>3</sub>-Fe<sub>2</sub>O<sub>3</sub> and modified with Cu exhibited the highest values of specific surface area. It should be also noted that despite  $S_{\text{BET}}$  was significantly improved, the increase was related mainly to the development of the external surface area. Both  $S_{\text{Micro}}$  and  $V_{\text{Micro}}$  were almost unchanged or even lower after modifications of bentonite. Therefore, all of the procedures performed on the aluminosilicate precursor resulted mainly in the development of new macro- and mesopores, which is in line with the results described basing on the isotherms obtained for the samples.

Table 3. Structural and textural features recognized from low-temperature N<sub>2</sub> sorption studies.

Sample code	$S_{\text{BET}}^a$ (m <sup>2</sup> · g <sup>-1</sup> )	$S_{\text{Ext}}^b$ (m <sup>2</sup> · g <sup>-1</sup> )	$S_{\text{Micro}}^b$ (m <sup>2</sup> · g <sup>-1</sup> )	$V_{\text{Micro}}^b$ (m <sup>3</sup> · g <sup>-1</sup> )	$V_{\text{Total}}^c$ (m <sup>3</sup> · g <sup>-1</sup> )	$V_{\text{Meso+Micro}}^d$ (m <sup>3</sup> · g <sup>-1</sup> )
Bent	50	34	16	0.008	0.131	0.123
H-Bent	290	263	27	0.012	0.844	0.832
H-Bent-Al	241	228	13	0.005	0.781	0.776
H-Bent-AlFe	283	265	18	0.008	0.784	0.776
H-Bent-Al-Cu	241	229	12	0.005	0.776	0.771
H-Bent-AlFe-Cu	298	273	25	0.011	1.203	1.192
Na-Bent	280	264	16	0.007	0.785	0.778
Na-Bent-Al	250	239	11	0.004	0.833	0.829
Na-Bent-AlFe	242	234	9	0.003	0.690	0.687
Na-Bent-Al-Cu	242	234	8	0.003	0.830	0.827
Na-Bent-AlFe-Cu	251	244	7	0.002	0.747	0.745

<sup>a</sup> Surface area determined by BET method.

<sup>b</sup> Micropore surface area, external surface area, and micropore volume determined by *t*-plot.

<sup>c</sup> Total pore volume at  $p/p_0 = 0.98$  m<sup>3</sup> · g<sup>-1</sup>;

<sup>d</sup>  $V_{\text{Micro+Meso}} = V_{\text{Total}} - V_{\text{Micro}}$ .

### 3.2.3. Crystal structure

X-ray diffraction technique is an useful method to investigate the influence of the performed modifications on the crystalline structure of the materials and changes occurring after deposition of the active phase. XRD patterns obtained for H-Bent- and Na-Bent-supported samples are depicted in Fig.

4. The XRD results for non-modified bentonite indicated that the montmorillonite was the major phase of the material. The diffraction maximum located at  $2\theta$  of ca.  $5.7^\circ$  ( $d_{001} = 1.5$  nm) is attributed to the ordering of the clay layers and confirms the presence of the crystalline montmorillonite. Furthermore, the maxima at about  $20.9^\circ$  corresponds to the diffraction from (100) montmorillonite layers, while the reflection at ca.  $26.7^\circ$  is the main one reflecting the presence of quartz and other impurities in the material. The dual peak at ca.  $35.5^\circ$ , appearing in the patterns of Na-Bent-AlFe and Na-Bent-AlFe-Cu is assigned to the presence of  $\text{Fe}_2\text{O}_3$ . Interestingly, it is absent in the case of H-samples, confirming that formation of more bulky particles was promoted by sodium cations in the support. According to the general agreement, the basal spacing of the layered minerals depends on the thickness of the individual clay layer and the interlayer distance. Basing on the literature, the thickness of the montmorillonite layer is estimated to be around 0.96 nm. Therefore, the interlayer distance in the analyzed bentonite samples is approximately 0.54 nm, thus, typical for the hydrated aluminosilicates. XRD pattern obtained for acid activated, H-Bentonite is characterized by the lack of (001) reflection attributed to the ordering of the aluminosilicate layers. Therefore, pretreatment of the sample with mineral acid resulted in its delamination and arrangement of the individual layers in the form of so-called "house of cards" structure, characterized by non-parallel ordering. Similar effect was observed by Tjong et al. for acid-treated vermiculites. Taking into consideration disorganization of the aluminosilicate layers, it is difficult to assume how the introduced pillars influenced on the interlayer distance. Nevertheless, the results of ICP-OES clearly indicated that  $\text{Al}_2\text{O}_3$  as well as  $\text{Fe}_2\text{O}_3$  were successfully introduced into the structure of bentonite. What is important, the exchange with sodium prior to further modifications did not result in any significant changes of the crystalline structure. Furthermore, all of the samples exhibited almost identical XRD patterns, in which intensity of the reflections is significantly lower comparing to the raw clay. Hence, the performed modifications not only led to delamination of bentonite, but also decreased crystallinity of the material. However, the lack of diffraction maxima originating from copper oxide suggests that the species, even if present (see UV-Vis-DR studies) were well-dispersed between and on the surface of the disordered layers.

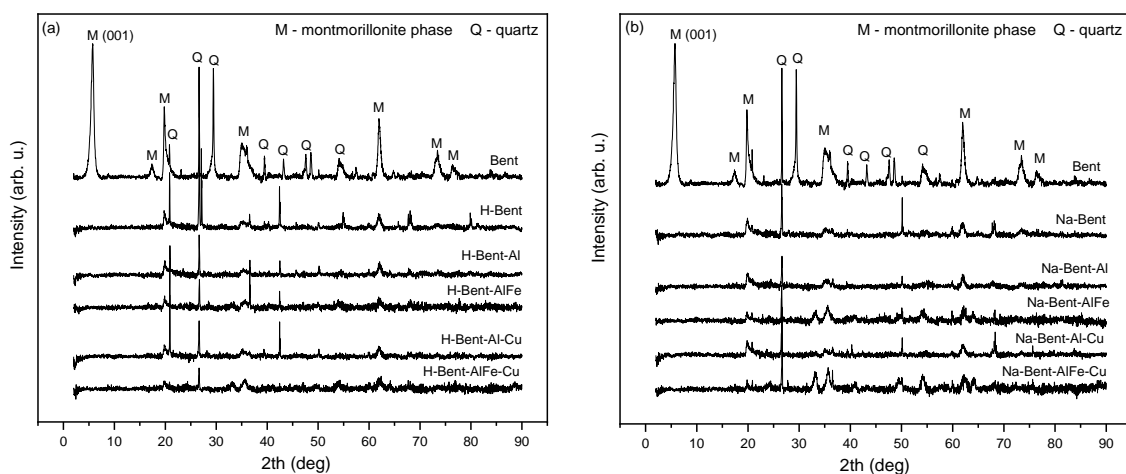


Fig. 4. XRD patterns obtained for a) H-bentonite-supported catalysts and (b) Na-bentonite-supported catalysts

### 3.2.4. Distribution of the active phase

UV-Vis-DR experiments were carried out in order to investigate the form and aggregation of Fe and Cu species in the modified bentonite. The recorded spectra, presented in Fig. 5., indicated that all of the samples exhibited strong absorption bands below 600 nm. According to the general agreement, the bands appearing in the region of 220-250 nm in the spectra of Fe-containing samples correspond to the charge transfer transition of  $\text{Fe}^{3+}$  in the tetrahedral coordination ( $\text{FeO}_4$ ). On the other and,  $\text{Fe}^{3+}$  in the octahedral coordination can be identified by the bands present within 260-270 nm. Furthermore, the octahedral  $\text{Fe}^{3+}$  cations in the small oligomeric clusters ( $\text{Fe}_x\text{O}_y$ ) give raise to the absorption bands between 350 and 400 nm, while the peaks in the range of 400-550 nm indicate bulky particles of  $\text{Fe}_2\text{O}_3$ . Therefore, the results presented in Fig. 5. confirm that iron present naturally in the non-modified bentonite takes the form of  $\text{Fe}^{3+}$  cations in the octahedral coordination (245 nm) and oligomeric species

(365 nm). After pretreatment with the mineral acid, intensity of the bands given by iron species significantly decreased, as the result of leaching and elimination of  $\text{Fe}^{3+}$  from the layered structure. The obtained outcome is in line with ICP-OES, which indicated considerable decrease of Fe concentration in the sample. Obviously, ion-exchange procedure with sodium, nor pillaring with  $\text{Al}_2\text{O}_3$  did not change concentration of iron in the samples, thus, the spectra obtained for H-Bent, Na-Bent and the  $\text{Al}_2\text{O}_3$ -intercalated materials were almost identical. The noticeable difference in the shape of the spectra can be observed only after pillaring with  $\text{Al}_2\text{O}_3\text{-Fe}_2\text{O}_3$  and modification with copper. First of all, introduction of iron oxide into the layered structure of bentonite resulted in the drastically increased intensity of the bands ascribed to all types of iron species. What is important, Na-Bent-AlFe exhibited broader band assigned to isolated iron monomers (below 250 nm) comparing to H-Bent-AlFe. Additionally, the band with the peak located at 520 nm, suggests that the sodium-modified sample contains more aggregated  $\text{Fe}_2\text{O}_3$  particles comparing to the protonated one.

In general, in the case of the materials modified with copper, UV-Vis-DR spectra show strong absorption bands below 400 nm. The region in the range of 200-250 nm corresponds to  $\text{Cu}^{2+}$  monomers interacting with oxygen in the crystalline aluminosilicate structure, while the region of 250-400 nm is typical for oligomeric copper species [ $\text{Cu}^{2+}\text{-O}^{2-}\text{-Cu}^{2+}$ ]. It can be observed that introduction of copper slightly increased the intensity of the spectra recorded for the samples pillared with  $\text{Al}_2\text{O}_3$ . Therefore, very small amount of  $\text{Cu}^{2+}$  was successively deposited in the structure of the clay. On the contrary, the absorption bands of the materials pillared with aluminum and iron oxides were noticeably less intense after impregnation with Cu. Such effect can be explained by the occurrence of some interactions between iron and copper present simultaneously in the clay. It should be also noted that due to the overlapping of the bands assigned to Cu and Fe, it is difficult to assign the particular intensities to the specific species. However, due to very low concentration of copper, it is expected that the metal was present mainly in the form of isolated  $\text{Cu}^{2+}$  monomers.

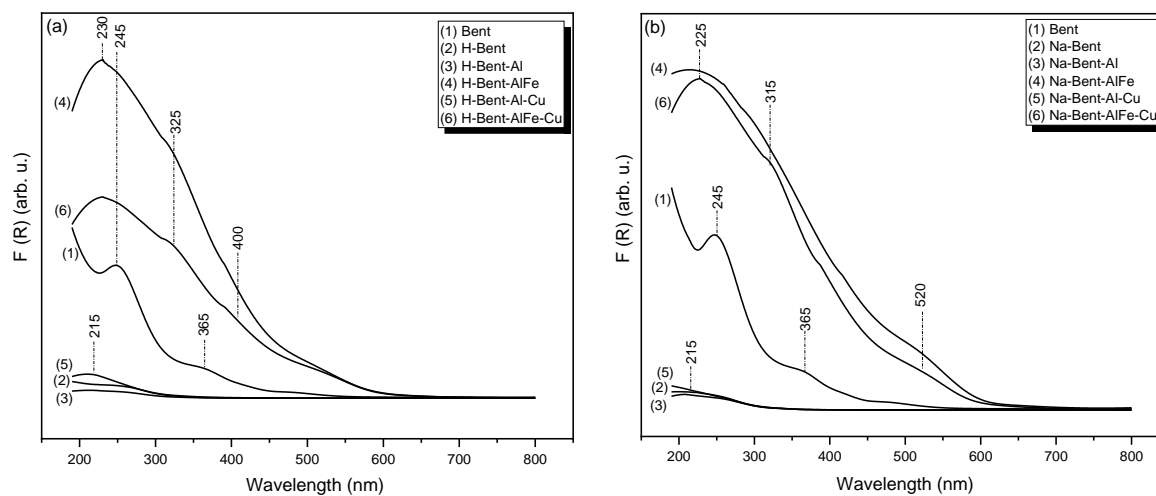


Fig. 5. UV-Vis-DR spectra recorded for a) H-bentonite-supported catalysts and (b) Na-bentonite-supported catalysts

#### 4. Conclusions

The samples of natural layered aluminosilicate, bentonite were modified with iron and copper and tested as the new, ecological-friendly catalyst of  $\text{NH}_3\text{-SCR}$ . In order to increase catalytic potential of the raw clay, bentonite was pretreated according to two routes: (1) pretreatment with mineral acid and intercalation with various pillars or (2) pretreatment with mineral acid, ion-exchange with sodium cations, and pillaring (identically to the route (1)). In order to reduce the number of synthesis steps, iron as the active phase was introduced into the structure of the materials in the form of pillars, co-existing with aluminum oxide. Both series of samples were additionally doped with copper in order to promote their low-temperature activity. The obtained results indicated that modification of the clay with acid resulted in disorganization of its layers, probable formation of so-called "house-of-cards" structure, and decreased crystallinity. However, the analysis of the textural parameters of the samples proved that

acid activation and intercalation significantly improved specific surface area and total pore volume, directly facilitating the diffusion of the reacting molecules through the aluminosilicate framework and adsorption on the active sites. The results of NH<sub>3</sub>-SCR catalytic tests indicated that the samples in which acid activation was followed by the exchange with sodium cations exhibited more stable NO conversion in the high temperature range comparing to H-Bent materials. The obtained result can be correlated with the beneficial speciation of the active phase in Na-Bent samples, identified by UV-Vis-DR. All in all, it was proved that iron oxide can be successfully introduced into the layered structure of bentonite during the pillaring procedure. In our view, the proposed solution is especially attractive for the industries located in the regions abundant in bentonite deposits, which would significantly limit the cost of transport of the catalyst precursor. Another great advantage of bentonite-supported catalysts is related to the usage of the existing natural clay, instead of the preparation of the new chemical catalytic system, as in the case of the vanadia-titania catalyst. Considering the application prospect of the proposed solution, it should be also emphasized that bentonite-supported catalysts modified with transition metals are much more eco-friendly, comparing to the commercial system containing toxic vanadium. To sum up, we have confirmed that natural bentonite is very promising precursor of the alternative, ecological-friendly catalysts for NH<sub>3</sub>-SCR process

### Acknowledgments

Agnieszka Szymaszek-Wawryca gratefully acknowledges the financial support of the research from National Science Centre Grant, Preludium 19 (no. 2020/37/N/ST5/00186). Monika Motak and Bogdan Samojeden would like to kindly acknowledge AGH Grant "Excellence Initiative - Research University" for the financial support. Urbano Díaz acknowledges the support from the Government of Spain through the project PID2020-112590GB-C21/AEI/10.13039/501100011033.

### References

- ADEYEMO, A. A., ADEOYE, I. O., BELLO, O. S. 2017. *Adsorption of dyes using different types of clay: a review*. Applied Water Science, 7(2), 543-568.
- ARUS V.A., NOUSIR S., SENNOUR R, SHIAO T.C., NISTOR I.D, ROY R., AZZOUZ A., 2018. *Intrinsic affinity of acid-activated bentonite towards hydrogen and carbon dioxide*. Int. J. Hydrog. Energy 43(16), 7964-7972.
- BARTH, J., JENTYS, A., KORNIATOWSKI, J., LERCHER, J. A., AL, O., O, M. AL. 2004. *Control of Acid - Base Properties of New Nanocomposite Derivatives of MCM-36 by Mixed Oxide Pillaring*. 8, 724-730.
- BERGAYA, F., AOUAD, A., MANDALIA, T. 2006. Chapter 7.5 *Pillared Clays and Clay Minerals*. Developments in Clay Science, 1(C), 393-421.
- BERTELLA, F., PERGHER, S. B. C. 2015. *Pillaring of bentonite clay with Al and Co*. Microporous and Mesoporous Materials, 201(C), 116-123.
- BOROŃ, P., CHMIELARZ, L., DZWIGAJ, S. 2015. *Influence of Cu on the catalytic activity of FeBEA zeolites in SCR of NO with NH<sub>3</sub>*. Applied Catalysis B: Environmental, 168-169, 377-384.
- BRANDENBERGER S., KRÖCHER O., TISSLER A., ALTHOFF R., 2010. *The determination of the activities of different iron species in Fe-ZSM-5 for SCR of NO by NH<sub>3</sub>*. Appl. Catal. B Environ. 95, 348-357.
- CARRIAZO, J. G., CENTENO, M. A., ODRIOZOLA, J. A., MORENO, S., MOLINA, R. 2007. *Effect of Fe and Ce on Al-pillared bentonite and their performance in catalytic oxidation reactions*. Applied Catalysis A: General (Vol. 317, Issue 1, pp. 120-128).
- CATRINESCU, C., ARSENE, D., APOPEI, P., TEODOSIU, C. 2012. *Degradation of 4-chlorophenol from wastewater through heterogeneous Fenton and photo-Fenton process, catalyzed by Al-Fe PILC*. Applied Clay Science, 58(3), 96-101.
- CHEN, D., CEN, C., FENG, J., YAO, C., LI, W., TIAN, S., XIONG, Y. 2016. *Co-catalytic effect of Al-Cr pillared montmorillonite as a new SCR catalytic support*. Journal of Chemical Technology and Biotechnology, 91(11), 2842-2851.
- CHLUBNÁ, P., ROTH, W. J., ZUKAL, A., KUBU, M., J., J. P. 2012. *Pillared MWW zeolites MCM-36 prepared by swelling MCM-22P in concentrated surfactant solutions*. Catalysis Today, 179, 35-42.
- CHMIELARZ, L., KOWALCZYK, A., MICHALIK, M., DUDEK, B., PIWOWARSKA, Z., MATUSIEWICZ, A. 2010. *Acid-activated vermiculites and phlogophites as catalysts for the DeNOx process*. Applied Clay Science, 49(3), 156-162.

- CHMIELARZ, L., KOWALCZYK, A., SKOCZEK, M., RUTKOWSKA, M., GIL, B., NATKAŃSKI, P., RADKO, M., MOTAK, M., DĘBEK, R., RYCZKOWSKI, J. 2018. *Porous clay heterostructures intercalated with multicomponent pillars as catalysts for dehydration of alcohols*. Applied Clay Science, 160(July 2017), 116–125.
- CHMIELARZ, L., KOWALCZYK, A., WOJCIECHOWSKA, M., BOROŃ, P., DUDEK, B., MICHALIK, M. 2014. *Montmorillonite intercalated with SiO<sub>2</sub>, SiO<sub>2</sub>-Al<sub>2</sub>O<sub>3</sub> or SiO<sub>2</sub>-TiO<sub>2</sub> pillars by surfactant-directed method as catalytic supports for DeNOx process*. Chemical Papers, 68(9), 1219–1227.
- CHMIELARZ, L., KUŚTROWSKI, P., PIWOWARSKA, Z., MICHALIK, M., DUDEK, B., DZIEMBAJ, R. 2009. *Natural micas intercalated with Al<sub>2</sub>O<sub>3</sub> and Modified with transition metals as catalysts of the selective oxidation of ammonia to nitrogen*. Topics in Catalysis (Vol. 52, Issue 8, pp. 1017–1022).
- CHMIELARZ, L., RUTKOWSKA, M., JABŁOŃSKA, M., WĘGRZYN, A., KOWALCZYK, A., BOROŃ, P., PIWOWARSKA, Z., MATUSIEWICZ, A. 2014. *Acid-treated vermiculites as effective catalysts of high-temperature N<sub>2</sub>O decomposition*. Applied Clay Science, 101, 237–245.
- DE OLIVEIRA, C. I. R., ROCHA, M. C. G., DA SILVA, A. L. N., Bertolino, L. C. 2016. *Characterization of bentonite clays from Cubati, Paraíba Northeast of Brazil*. Ceramica, 62(363), 272–277.
- GIL, A., KORILI, S. A., TRUJILLANO, R., VINCENTE, M. A. 2013. *Pillared Clays and Related Catalysts*.
- GRZYBEK, T. 2007. *Layered clays as SCR deNOx catalysts*. Catalysis Today, 119(1–4), 125–132.
- HAN, Z., YU, Q., LIU, J., ZUO, Z., LIU, K., XUE, Z., QIN, Q. 2019. *Chromium, iron or zirconium oligomer cations pillared interlayered montmorillonite carrier supported MnOx for low-temperature selective catalytic reduction of NOx by NH<sub>3</sub> in metallurgical sintering flue gas*. Energy Sources, Part A: Recovery, Utilization and Environmental Effects.
- HART, M. P., BROWN, D. R. 2004. *Surface acidities and catalytic activities of acid-activated clays*. Journal of Molecular Catalysis A: Chemical, 212(1–2), 315–321.
- IBRAHIM, Y., MOHAMAD HARDYMAN, B., JAMES, M. 2021. *Assessment of copper-iron catalyst supported on activated carbon for low-temperature nitric oxide reduction by hydrogen*. IOP Conference Series: Earth and Environmental Science, 765(1).
- KOMADEL, P. 2016. *Acid activated clays: Materials in continuous demand*. Applied Clay Science, 131, 84–99.
- KUMAR, A., LINGFA, P. 2020. *Sodium bentonite and kaolin clays: Comparative study on their FT-IR, XRF, and XRD*. Materials Today: Proceedings, 22, 737–742.
- LIN, Z., YANG, Y., LIANG, Z., ZENG, L., ZHANG, A. 2021. *Preparation of chitosan/calcium alginate/bentonite composite hydrogel and its heavy metal ions adsorption properties*. Polymers, 13(11).
- LUCJAN CHMIELARZ, WOJCIECHOWSKA, M., RUTKOWSKA, M., ADAMSKI, A., WĘGRZYN, A., KOWALCZYK, A., DUDEK, B., BOROŃ, P., MICHALIK, M., MATUSIEWICZ, A. 2012. *Acid-activated vermiculites as catalysts of DeNOx process*. Catalysis Today, 191, 25–31.
- MAGED, A., KHARBISH, S., ISMAEL, I. S., BHATNAGAR, A. 2020. *Characterization of activated bentonite clay mineral and the mechanisms underlying its sorption for ciprofloxacin from aqueous solution*. Environmental Science and Pollution Research, 27(26), 32980–32997.
- MOTAK, M. 2008. *Montmorillonites modified with polymer and promoted with copper as DeNOx catalysts*. Catalysis Today (Vol. 137, Issues 2–4, pp. 247–252).
- MUÑOZ, H. J., BLANCO, C., GIL, A., VICENTE, M. ÁNGEL, GALEANO, L. A. 2017. *Preparation of Al/Fe-pillared clays: Effect of the starting mineral*. In Materials (Vol. 10, Issue 12).
- ÖZCAN, A. S., ÖZCAN, A. 2004. *Adsorption of acid dyes from aqueous solutions onto acid-activated bentonite*. Journal of Colloid and Interface Science (Vol. 276, Issue 1, pp. 39–46).
- PALUSZKIEWICZ, C., HOLTZER, M., BOBROWSKI, A. 2008. *FTIR analysis of bentonite in moulding sands*. Journal of Molecular Structure, 880(1–3), 109–114.
- RAHKAMAA-TOLONEN, K., MAUNULA, T., LOMMA, M., HUUHTANEN, M., KEISKI, R.L., 2005. *The effect of NO<sub>2</sub> on the activity of fresh and aged zeolite catalysis in the NH<sub>3</sub>-SCR reaction*. Catal. Today 100, 217–222.
- RHODES, C. N., BROWN, D. R. 1995. *Autotransformation and ageing of acid-treated montmorillonite catalysts: A solid-state <sup>27</sup>Al NMR study*. Journal of the Chemical Society, Faraday Transactions, 91(6), 1031–1035.
- SHATTAR, S. F. A., ZAKARIA, N. A., FOO, K. Y. 2020. *One step acid activation of bentonite derived adsorbent for the effective remediation of the new generation of industrial pesticides*. Scientific Reports, 10(1), 1–13.
- ZHIHAO, S., SHUMING, W., HAN, W., YONGCHAO, M., XIAO, W., SHENGBING, M., QICHENG, F. 2023. *Effect of dissolved components of malachite and calcite on surface properties and flotation behavior*. International Journal of Minerals, Metallurgy and Materials, 30, 1297–1309.

- SKALSKA, K., MILLER, J. S., Ledakowicz, S. 2010. *Trends in NO<sub>x</sub> abatement: A review*. Science of the Total Environment (Vol. 408, Issue 19, pp. 3976–3989).
- STAWIŃSKI, W., FREITAS, O., CHMIELARZ, L., WĘGRZYN, A., KOMĘDERA, K., BŁACHOWSKI, A., FIGUEIREDO, S. 2016. *The influence of acid treatments over vermiculite based material as adsorbent for cationic textile dyestuffs*. Chemosphere, 153, 115–129.
- SZYMASZEK, A., KUBEŁ, M., SAMOJEDEN, B., MOTAK, M. 2020. *Modified bentonite-derived materials as catalysts for selective catalytic reduction of nitrogen oxides*. Chemical and Process Engineering (Vol. 2020, Issue 1, pp. 13–24).
- SZYMASZEK, A., SAMOJEDEN, B., MOTAK, M. (2020). *The Deactivation of Industrial SCR Catalysts – A Short Review*. Energies, 13(15), 3870.
- TJONG, S.C., MENG, Y.Z. 2003, *Impact-modified polypropylene/vermiculite nanocomposites*. J. Polym. Sci. B Polym. Phys., 41, 2332-2341.
- WATT, J. A. J., BURKE, I. T., EDWARDS, R. A., MALCOLM, H. M., MAYES, W. M., OLSZEWSKA, J. P., PAN, G., GRAHAM, M. C., HEAL, K. V., ROSE, N. L., TURNER, S. D., SPEARS, B. M. 2018. *Vanadium: A Re-Emerging Environmental Hazard*. Environmental Science and Technology, 52(21), 11973–11974.
- WENJUAN, Z., BIN, Y., YAHUI, Y., QICHENG, F., DIANWEN, L. 2023. *Synergistic activation of smithsonite with copper-ammonium species for enhancing surface reactivity and xanthate adsorption*. International Journal of Mining Science and Technology, 33(4), 519-527.
- YAMAMOTO, K., IKEDA, T., TSUKAMOTO, Y. 2021. *Synthesis of a novel crystalline organic–inorganic hybrid material KCS-11, an ethanol-breathing pseudoporous layered aluminosilicate*. Materials Letters, 288, 129332.
- ZANIN, E., SCAPINELLO, J., DE OLIVEIRA, M., RAMBO, C. L., FRANSCESCON, F., FREITAS, L., DE MELLO, J. M. M., FIORI, M. A., OLIVEIRA, J. V., DAL MAGRO, J. 2017. *Adsorption of heavy metals from wastewater graphic industry using clinoptilolite zeolite as adsorbent*. Process Safety and Environmental Protection, 105, 194–200.
- ZHANG, T., LIU, J., WANG, D., ZHAO, Z., WEI, Y., CHENG, K., JIANG, G., DUAN, A. (2014). *Selective catalytic reduction of NO with NH<sub>3</sub> over HZSM-5-supported fe-cu nanocomposite catalysts: The fe-cu bimetallic effect*. Applied Catalysis B: Environmental (Vols. 148–149, pp. 520–531).
- ZHOU, C. H. 2011a. *An overview on strategies towards clay-based designer catalysts for green and sustainable catalysis*. Applied Clay Science, 53(2), 87–96.
- ZHOU, C. H. 2011b. *An overview on strategies towards clay-based designer catalysts for green and sustainable catalysis*. Applied Clay Science, 53(2), 87–96.
- ZI, W. W., ZHANG, J., CAI, X. S., JIAO, F., DU, H. BIN. 2020. *Synthesis and characterization of a layered aluminosilicate NUD-11 and its transformation to a 3D stable zeolite*. Dalton Transactions, 49(33), 11682–11688.